RSC Advances

ROYAL SOCIETY OF CHEMISTRY

PAPER

View Article Online
View Journal | View Issue

Cite this: *RSC Adv.*, 2022, **12**, 29697

Composite protective effect of benzotriazole and 2-mercaptobenzothiazole on electroplated copper coating

Huimin Chen,[a] Shuaixing Wang,*[ab] Zhixiang Liao,[a] Shusen Peng[a] and Nan Du[ab]

Benzotriazole (BTAH) and 2-mercaptobenzothiazole (MBT) are mixed to passivate electroplated copper coatings. The growth process of passive films is comprehensively analyzed from the surface potential, microstructure and chemical composition by potential–time curve, FESEM and XPS. Meanwhile, the corrosion resistance of copper coatings with different passivation treatments is evaluated by potentiodynamic polarization curves and electrochemical impedance spectroscopy. During the composite passivation process of BTAH and MBT, the copper coating undergoes the following steps: chemical dissolution of the copper coating, preferential adsorption of MBT, formation of Cu(I)–BTA complex film and Cu_2O, and synergistic growth of Cu(I)–BTA and Cu(I)–MBT. A protective film with a thickness of about 233 nm, containing the inner layer of BTA–Cu(I) and MBT–Cu(I) and the outer layer of MBT–Cu(I) and Cu_2O, is formed on the copper coating after composite passivation. The composite passivation film significantly improves the corrosion resistance of copper coatings, and its corrosion inhibition efficiency for copper coatings reaches 90.7%, which is far better than that produced by using BTAH or MBT alone.

Received 29th August 2022
Accepted 9th October 2022

DOI: 10.1039/d2ra05411f

rsc.li/rsc-advances

Open Access Article. Published on 25 October 2022. Downloaded on 1/31/2025 4:54:28 AM.
This article is licensed under a Creative Commons Attribution-NonCommercial 3.0 Unported Licence.

1 Introduction

Electroplated copper coatings are widely used for decoration, electrical conductivity, chemical heat treatment protection and other functional requirements. In general, copper has good corrosion resistance, but it is prone to severe corrosion in oxygen-containing oxidizing acids or solutions containing CN^- or NH_4^+.[1] In order to further improve the corrosion resistance of copper alloys or copper coatings, passivation is often used to protect them.[1–6] Currently, chromate is widely used to passivate copper plating in the aviation industry,[7,8] but it is necessary to develop a chromium-free passivation process due to the pollution of Cr(VI) to the environment.

Recently, some research has been carried out on the chromium-free passivation of copper alloys. Dodecanethiol (DT), benzothiazole (BT), benzotriazole (BTA or BTAH), 2-mercaptobenzothiazole (MBT), 2-mercaptobenzoxazole (MBO), methyl benzotriazole nitrile (TTA) and their derivatives are considered to be effective corrosion inhibitors for copper alloys,[9–13] and the self-assembled films formed by the chemical adsorption of these substances on the surface of copper alloys can provide good protection for copper alloys. Research has shown that BTA can form a Cu(I)–BTA complex film with Cu^+ on the copper surface to prevent copper corrosion,[10,11] however, it is easy to form an incomplete complex film and the protective effect is poor when BTA is used alone, and so it is often used in combination with other organic and inorganic additives. Studies determined that potassium sorbate, OP-10, molybdate and phosphate all showed good synergistic effects with BTAH.[14–18] BTAH alone protects copper from corrosion in sulfate solutions only in the potential range below 0.4 V (*vs.* SCE), but a mixture of potassium 2,4-hexadienoate and BTAH provides complementary and robust corrosion protection for copper over a wide potential range.[14] The combination of BTAH and molybdate promotes the formation of BTAH passivation film on copper, and shows better corrosion inhibition performance than single BTAH.[15] The corrosion inhibition effect of the mixture of BTA and Na_3PO_4 on copper in tetra-*n*-butylammonium bromide (TBAB) aerated aqueous solution is also better than that of BTA itself, and the anodic process of copper corrosion is significantly inhibited.[16] Besides, the combined action of BTA and TTA can form a denser passivation film on the surface of T2 copper, and the passivation effect of the compound on T2 copper is similar to that of chromate.[15]

In addition, some research has also shown that MBT has a different corrosion inhibition mechanism, which mainly prevents the corrosion of copper by adsorbing on the copper surface.[5,12,18–20] If BTAH is compounded with MBT, the inhibitory effect on the anodic and cathodic electrochemical processes of copper electrodes can be enhanced, and the corrosion inhibition effect on copper can be better. But little is known about the composite application of MBT and BTAH on copper surfaces. In addition, most of the existing studies are

[a]School of Materials Science and Engineering, Nanchang Hangkong University, Nanchang 330063, P. R. China. E-mail: wsxxpg@126.com; Tel: +86-791-86453250
[b]National Defense Key Discipline Laboratory of Light Alloy Processing Science and Technology, Nanchang Hangkong University, Nanchang 330063, P. R. China

© 2022 The Author(s). Published by the Royal Society of Chemistry

Open Access Article. Published on 25 October 2022. Downloaded on 1/31/2025 4:54:28 AM.
This article is licensed under a Creative Commons Attribution-NonCommercial 3.0 Unported Licence.

aimed at copper alloys, and there are few studies on the passivation of copper coatings. Only the literature [10] gives the relative inhibition efficiency of different inhibitors in protecting electroplated copper coatings in the order of DT > MBT > BT > BTA > imidazole (IMD). There is no literature about the composite application of MBT and BTAH on the surface of electroplated copper coatings, and the synergistic mechanism of the two is rarely mentioned.

Electroplated copper coatings often have different physical and chemical characteristics from copper alloys, the crystal grains of copper coatings reach the nanometer scale, and the copper coatings formed in the alkaline etidronic acid (HEDP) system in this study almost have a fully preferred orientation of (111) crystal plane, the adsorption and film-forming mechanism of thiols or thiazoles on the surface of the highly preferred nanocrystalline coating may be very different. Sugimasa *et al.* have found that the adsorption of BTA molecules on different Cu crystal planes is different, which adsorb in parallel on the surfaces of Cu(110) and (100), while stack vertically on Cu(111) to form molecular rows in an ordered manner.[21] Girllo *et al.* confirmed that both physisorption and chemisorption phases of BTAH are present on a Cu(111) single crystal, and an extended and highly ordered self-assembled metal–organic phase can be seen at saturation coverage and above.[22] Therefore, BTAH and MBT are used for composite passivation treatment of electroplated copper coating in this paper, and the reaction mechanism and growth process of the passivation film are comprehensively analyzed from the surface potential, microstructure and chemical composition of the film, and the synergistic passivation mechanism of the two is discussed. In addition, the corrosion resistance of the composite passivation-treated copper plating was evaluated by potentiodynamic polarization curves and electrochemical impedance spectroscopy (EIS). The research results can provide technical support for the protection of copper coatings, and also help to deepen the understanding of film-forming mechanism of imidazole and thiazole passivation films.

2 Experimental

2.1 Preparation of copper coating and passivation film

Q235 steel sheet of 20 mm × 30 mm was used in the experiment, whose main chemical composition (wt%) is 0.17–0.22 C, 0.035–0.05 S, ≤1.4 Mn, and balanced with Fe. Prior to electroplating copper, the samples are sequentially treated by the following steps: polishing with 2000# sandpaper, rinsing in deionized water, degreasing in an aqueous solution containing 60 g L^{-1} NaOH, 35 g L^{-1} $Na_3PO_4\cdot12H_2O$ and 30 g L^{-1} Na_2CO_3 at 60 °C for 3 min, rinsing in deionized water, pickling in 10 vol% H_2SO_4 solution at room temperature for 1 min and rinsing in deionized water. Afterwards, the samples are placed in an alkaline HEDP bath for copper electroplating at 55–60 °C. Where, the copper plating bath contains 14 g L^{-1} $Cu_2(OH)_2CO_3$, 90 g L^{-1} HEDP, 40 g L^{-1} K_2CO_3 and 0.4 g L^{-1} surfactant, and pH value is adjusted to 9–10 by KOH; the current density of 1.0 A dm^{-2}, and the plating time is 60 min to control the thickness of copper coating at about 20 μm.

The passivation of the copper coating is carried out in BTAH solution, MBT solution and the composite system of the two, respectively. Meanwhile, hexavalent chromium passivation is selected for comparison. Among them, the BTAH, MBT and chromate passivation processes are mainly from the literature. The composite passivation process is obtained by preliminarily mixing the components of the BTAH and MBT solution and optimizing them in the early stage. The specific process and solution composition are shown in Table 1.

2.2 Electrochemical test

The potential–time curves of copper plating samples in different passivation systems and the potentiodynamic polarization curves and EIS of passivated samples in 3.5 wt% NaCl are measured by an electrochemical workstation (Autolab PGSTAT 302 N). A three-electrode electrochemical cell is used, the working electrode is a copper-plated or passivated sample encapsulated by epoxy resin with the exposed area of 1 cm^2, the auxiliary electrode and the reference electrode is a platinum sheet and a saturated calomel electrode (SCE). All potentials in the paper are relative to SCE.

The test time of the potential–time curve is 20 min, and the temperature of passivation solution is 60 °C. Potentiodynamic polarization curves are tested from −1.0 V to 0.5 V (*vs.* SCE) at a scan rate of 1 mV s^{-1}. EIS tests are acquired at the open circuit potential (OCP) over the frequency range of 0.01 Hz–100 KHz using an AC signal amplitude of 10 mV. The tests are performed at 25 °C and repeated by three specimens to ensure the

Table 1 The solution composition and process parameters of different passivation technique

Passivation process	Solution composition	Temperature	Immersion time
Cr(VI) passivation[7,8]	120 g L^{-1} $Na_2Cr_2O_7\cdot2H_2O$ 5 g L^{-1} H_2SO_4 10 g L^{-1} NaCl	25–30 °C	10–15 s
BTAH passivation[17]	4 g L^{-1} BTAH	55–60 °C	10 min
MBT passivation[5,12]	0.5 g L^{-1} MBT 4 g L^{-1} $Na_3PO_4\cdot12H_2O$	55–60 °C	10 min
BTAH + MBT passivation	4 g L^{-1} BTAH 0.5 g L^{-1} MBT 4 g L^{-1} $Na_3PO_4\cdot12H_2O$ 4 g L^{-1} sodium dodecyl sulfate	55–60 °C	10 min

 © 2022 The Author(s). Published by the Royal Society of Chemistry

reliability of the results. The equivalent circuits are fitted using the Zsimpwin software. Besides, the polarization curve is fitted according to Tafel extrapolation method, and the corrosion current density (i_{corr}) and the corrosion potential (E_{corr}) are obtained, the corrosion inhibition rate (η) can be measured by eqn (1).[3]

$$\eta = \frac{{i_{corr}}^0 - i_{corr}}{{i_{corr}}^0} \quad (1)$$

where, ${i_{corr}}^0$ and i_{corr} are the corrosion current of the samples before and after passivation treatment, respectively.

2.3 Microstructure and composition analysis

The surface morphologies of different passivation films are observed by a field emission scanning electron microscope (FESEM, Nova Nano SEM450). The elemental composition and valence state of the passive film are analyzed by X-ray photoelectron spectroscopy (XPS, Axis Ultra DLD) with a standard Al Ka X-ray source (1486.6 eV) and a hemispherical analyzer. Besides, Ar^+ sputtering is used for etching, the etching energy and the etching rate is 5 keV and 20 nm min^{-1}, respectively.

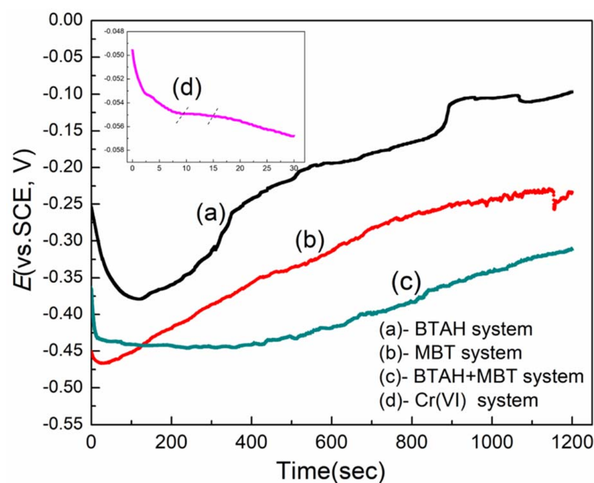

Fig. 1 Potential–time curves of electroplated copper coating in different passivation systems: (a) BTAH; (b) MBT; (c) BTAH + MBT; (d) chromate solution.

3 Results and discussion

3.1 Potential variation of copper coatings during immersion in different passivation systems

Fig. 1 gives the potential–time curves of electroplated copper coatings immersed in different passivation systems. In the single BTAH or MBT passivation system, the surface potential of the copper coating first decreases rapidly and then increases slowly, but the potential growth rate and final stable potential of the two are different. The initial potential of the copper coating in the BTAH system is −0.255 V, which decreased to −0.378 V at about 125 s, then slowly increased and tend to be stabilized after 850 s. In the MBT system, the potential of copper coating decreased rapidly from −0.451 V to −0.466 V within 30 s and then the potential gradually increased, but did not reach a stable state within 20 min. The potential change law of copper coating is slightly different in the composite passivation system of BTAH and MBT. The initial potential of the copper coating is −0.364 V, which is between that in the single BTAH or MBT systems. Although the potential of the copper coating also decreased first in this system, the rate of decrease is significantly faster with a decrease of 65 mV within 15 s, after then it entered a longer period of potential stabilization zone, and the potential began to slowly increase after 10 min.

It is generally believed that the initial potential of the copper coating is related to the passivation system. The subsequent decay of the potential is mainly attributed to the active dissolution of copper and the oxides on its surface.[5,23] The dissolution reaction speed and the reduction magnitude of potential are related to the speed of the formation of passivation film on the surface. Researches have confirmed that BTAH can form a complex protective film of Cu(I)–BTA on the copper surface, but this reaction can only occur when the concentration of Cu^+ reaches a certain level.[10,11,15,16] As shown in Fig. 1, the dissolution reaction of copper coating lasted for a long time in the BTAH system, and the complex film began to gradually form after 127 s. However, MBT mainly protects the copper coating by chemical adsorption.[5,12,18–20] The hydrogen atoms on the sulfhydryl groups of MBT molecules can be dissociated in water.[18,24] As soon as the copper plating layer is immersed in the MBT solution, the sulfur atoms immediately chemically adsorb with the copper and form a firm adsorption layer, so the potential starts to increase slowly after a small decrease. For the composite system of BTAH and MBT, the MBT adsorption layer may be preferentially formed on the surface of copper coating, but the initial adsorption layer is not complete. BTAH molecules may still react with Cu^+ generated by the dissolution of copper coating to form a Cu(I)–BTA protective film. The balance between the dissolution of Cu^+ and the film formation makes the overall potential relatively stable at this time. With the increase of the coverage of MBT adsorption layer and the Cu(I)–BTA protective film, the dissolution reaction of copper is difficult to occur, and the adsorption of MBT gradually becomes dominant. After that, the overall potential increases until the adsorption is saturated.

In addition, Fig. 1d shows that the potential change trend of copper coating in hexavalent chromate solution is quite different from other systems. The open circuit potential shows a downward trend within 30 s, but is in the plateau region within 10–15 s. The analysis shows that the dissolution of copper coating in the acidic chromate solution leads to a sharp drop in the potential within 0–3 s. Subsequently, the reduction of hexavalent chromium occurs on the electrode surface and a passivation film is formed,[7,8] which reduces the decrease rate of the potential. In 10–15 s, the existence of passivation film effectively inhibits the occurrence of dissolution and hydrogen evolution, so the potential is relatively stable. However, after a long time of immersion, the corrosion rate of chromate solution on the film increases and the potential decreases again.

Open Access Article. Published on 25 October 2022. Downloaded on 1/31/2025 4:54:28 AM. This article is licensed under a Creative Commons Attribution-NonCommercial 3.0 Unported Licence.

Open Access Article. Published on 25 October 2022. Downloaded on 1/31/2025 4:54:28 AM.
This article is licensed under a Creative Commons Attribution-NonCommercial 3.0 Unported Licence.

3.2 Microstructure of copper coatings under different passivation conditions

Fig. 2a and b are the surface SEM image and XRD spectrum of the copper coating prepared in the alkaline HEDP plating system, respectively. It can be seen that the copper coating is fine and uniform, and presents an obvious preferred orientation at (111) crystal plane. According to the Debye–Scherrer formula,[23] the average grain size of the coating is calculated and about 47–52 nm. Fig. 2d–l are the surface microstructure of copper coatings passivated for different times in BTAH, MBT and BTAH + MBT systems, respectively. The surface morphology is almost indistinguishable from the original copper coating when it is passivated in the BTAH system for 20 s, as shown in Fig. 2d. Cu–BTA complex products begin to appear on the surface of the coating after 125 s (Fig. 2e), the complexation products continued to increase with the prolongation of passivation time, but the copper coating is not completely covered by 10 min (Fig. 2f). In the MBT system, obvious adsorbates appear on the surface of copper coating after only 20 s for passivation (Fig. 2g), and the coverage of the adsorption layer increases with time, but the density of the simple adsorption layer is not high, and a few holes are present on the surface of the film (Fig. 2i).

In the composite system of BTAH and MBT, a small amount of adsorbate also exists on the surface of the film after passivation for 20 s, but it is slightly lower than that of MBT passivation film, seen in Fig. 2j. Subsequently, the Cu–BTA complex product film and the MBT adsorption film are continuously formed and gradually covered the entire coating under the synergistic effect of the two substances. A complete and dense passivation film is formed on the surface after 10 min, obvious holes are absent on the surface. The variation law of the film surface structure in different passivation systems also favorably confirms the discussion on the potential–time correlation of different systems. Besides, Fig. 2c shows the surface SEM image of copper coatings passivated in the chromate system for 15 s. The chromate passivation film is significantly different from other films, and the surface exhibits a network-like microcrack structure, which may be mainly attributable to the tensile stress developed in the coating during the chromating and drying process.[7,25]

Besides, Fig. 3 gives the cross-sectional morphologies of the passivation films obtained in different systems. It can be seen

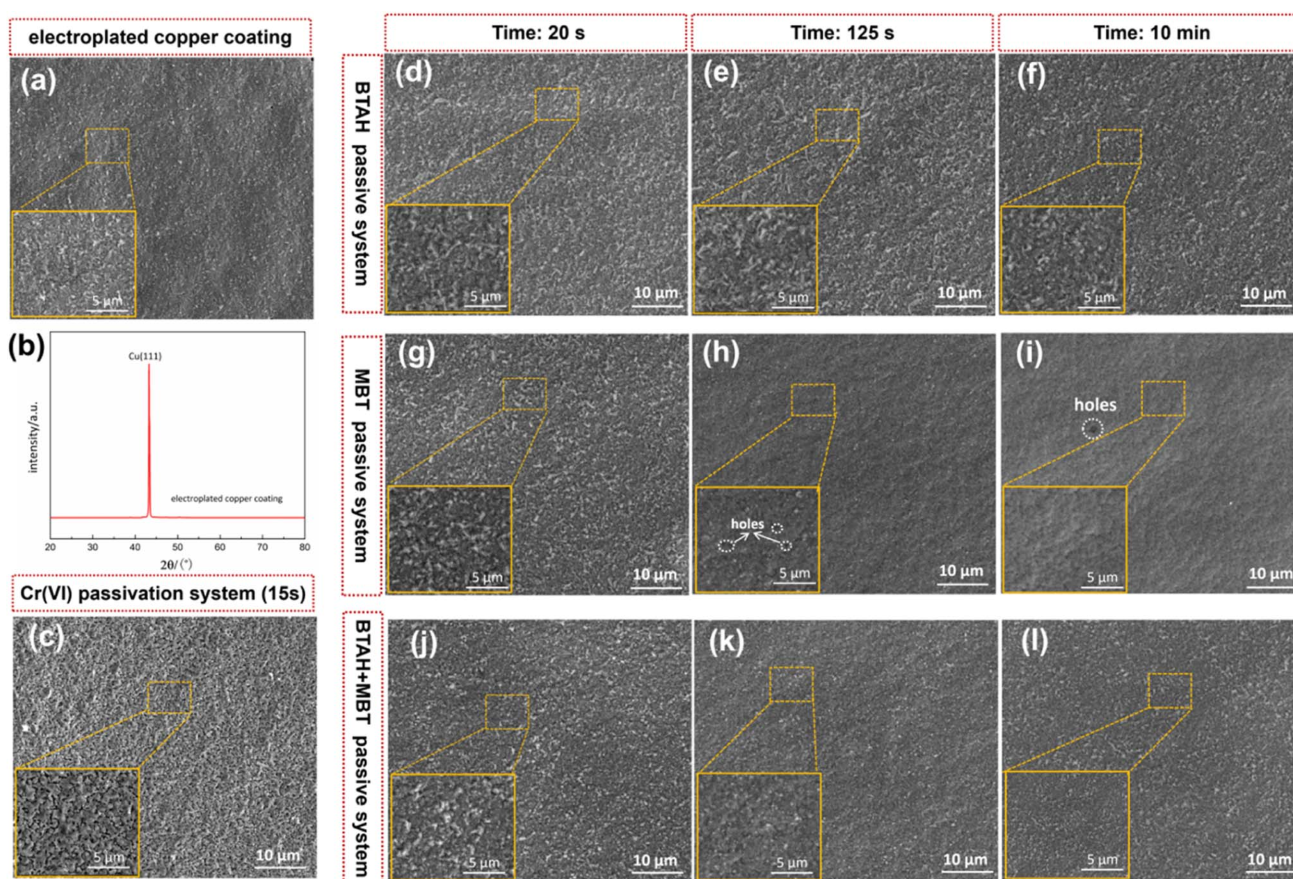

Fig. 2 Surface morphologies of electroplated copper coating treated in different passivation systems for different times. (a): SEM image of electroplated copper coating; (b): XRD pattern of electroplated copper coating; (c): SEM image of copper coating by hexavalent chromium passivation for 15 s; (d)–(f): SEM image of copper coating by BTAH passivation for 20 s, 125 s and 10 min; (g)–(i): SEM image of copper coating by MBT passivation for 20 s, 125 s and 10 min; (j)–(l): SEM image of copper coating by BTAH + MBT passivation for 20 s, 125 s and 10 min.

© 2022 The Author(s). Published by the Royal Society of Chemistry

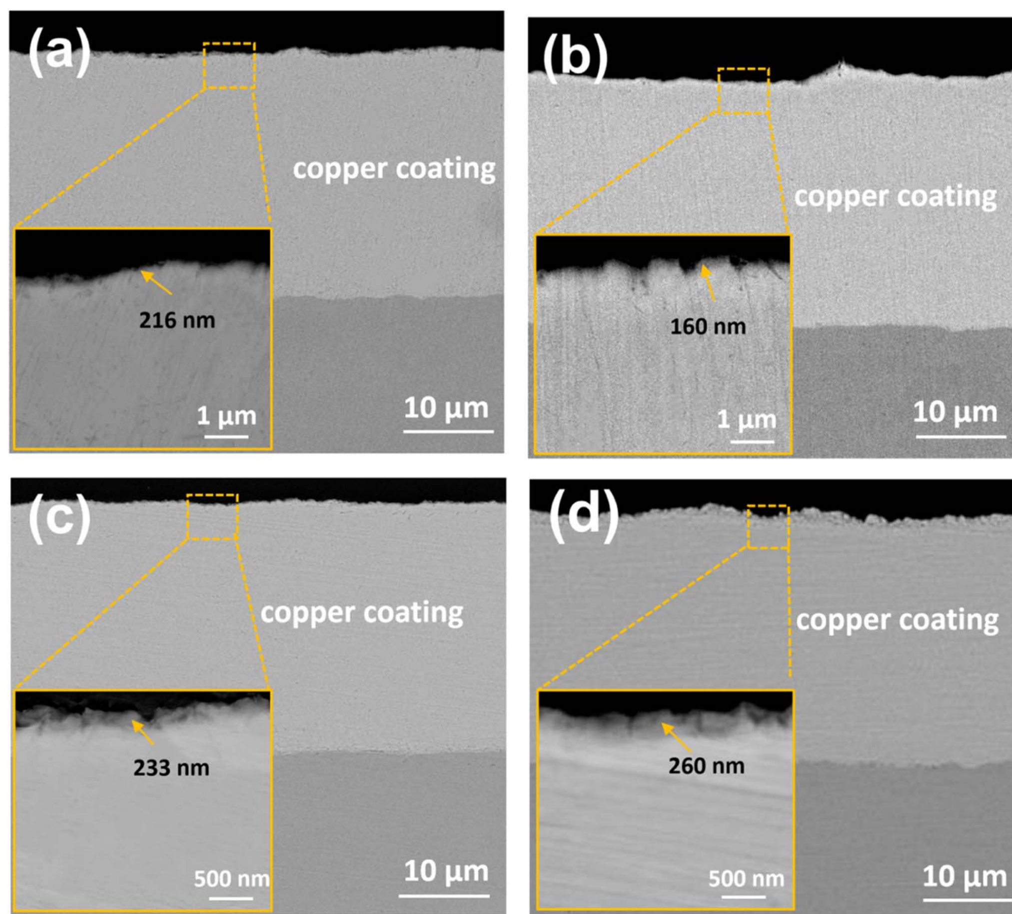

Fig. 3 Cross-sectional morphologies of electroplated copper coating treated in different passivation systems: (a) BTAH; (b) MBT; (c) BTAH + MBT; (d) chromate solution.

Open Access Article. Published on 25 October 2022. Downloaded on 1/31/2025 4:54:28 AM.
This article is licensed under a Creative Commons Attribution-NonCommercial 3.0 Unported Licence.

that the thickness of all copper coating is about 20 µm, which can effectively avoid the influence of copper coating. There are some differences in the structure and thickness of the passivation films obtained in different passivation systems. As shown in Fig. 3d, an obvious film with a thickness of about 260 nm is formed on the surface of copper coating after chromate passivation. Some network microcracks can also be seen from the cross section of the film, which corresponds to the surface morphology (Fig. 2c). After passivation by BTAH, a complex product film is also formed on the surface of copper coating, and the thickness of film can be determined to be about 216 nm by high-magnification SEM image, as shown in Fig. 3a. However, the structure of MBT passivation film on the surface of copper coating is not obvious, and its thickness is vaguely 160 nm. The reason may be that MBT mainly forms a film on the copper coating surface by adsorption,[18–20] and the adsorption degree of organic matter is limited, which is not obvious under the electron microscope test. In addition, it can be seen from Fig. 3c that a thicker passivation film with a obvious structure is formed on the coating surface after composite passivation, and the film thickness is about 233 nm. It can also be roughly seen that the continuity of the outer surface of the film is slightly poor, and the interface near the copper coating is denser.

3.3 Analysis of the surface composition of copper coatings under different passivation conditions

Fig. 4a presents the XPS survey spectra of the passivation film treated for 10 min in BTAH + MBT system. The high-resolution spectra of C 1s, O 1s, S 2p and N 1s are shown in Fig. 4b–f, respectively. As shown in Fig. 4a, C, O, Cu, S and N are present on the surface of the BTAH + MBT composite passivation film, but the characteristic peak of P 2p is absent. After etching by Ar^+ sputtering for 10 min, the surface conductivity of the sample is improved, and the peak signal is significantly enhanced, but S and N elements still exists on the surface of the film, which also indicates the thickness of the passivation film are greater than 200 nm.

Fig. 4b shows that the C 1s spectrum of the composite passivation film can be curve-fitted into three peak with binding energies at about 284.8 eV, 285.6 eV and 286.5 eV, which are almost identical to the shape and position of C 1s spectral peak for MBT powder, corresponding to C═S and C═N (C3), C–S and C–N (C2), and the remaining atoms in the benzene ring (C1).[5,26–28] Therefore, it can be considered that the C atom does not participate in the binding of Cu. As shown in Fig. 4c, the O 1s spectrum consists of two peaks. The main peak at 532.8 eV (O1) originates from the water molecules adsorbed on the surface, which may stay on the surface of passivation film by

Open Access Article. Published on 25 October 2022. Downloaded on 1/31/2025 4:54:28 AM. This article is licensed under a Creative Commons Attribution-NonCommercial 3.0 Unported Licence.

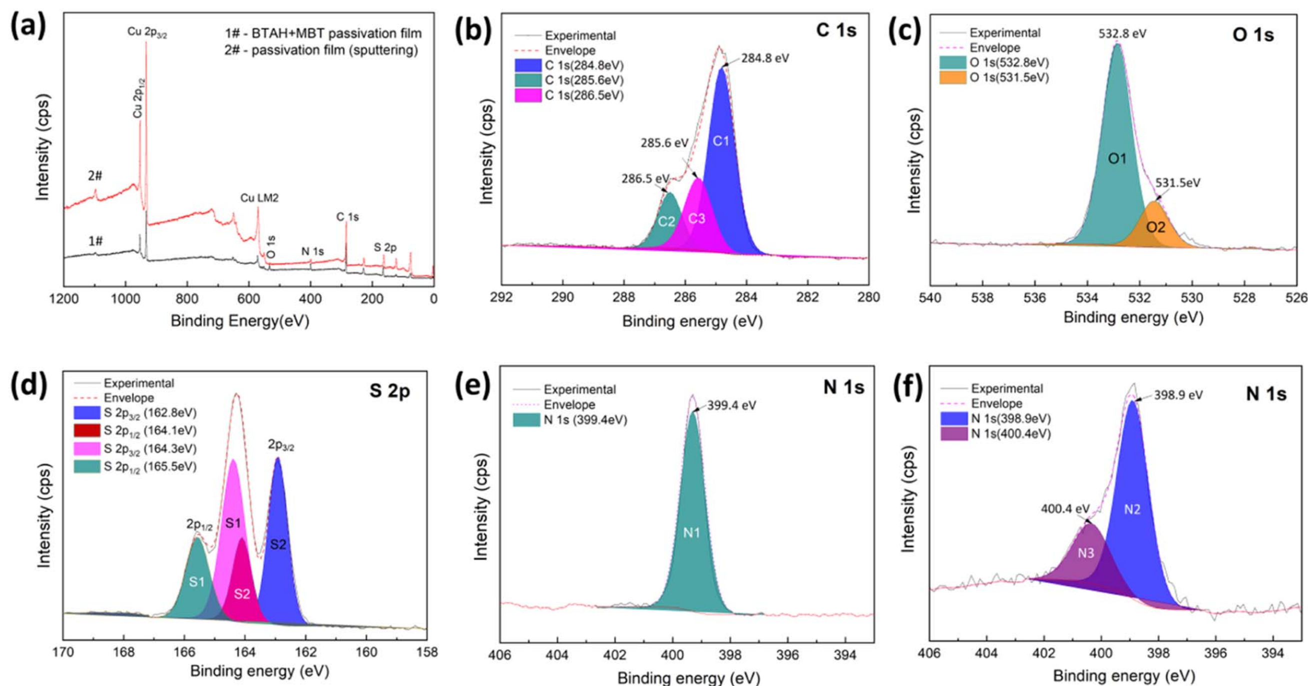

Fig. 4 X-ray photoelectron spectroscopy of BTAH + MBT passivation film on the copper coating surface. (a): Full-scale spectra of passivation film before and after etching; (b)–(e): high-resolution spectra of C 1s, O 1s, S 2p and N 1s for unetched passivation film; (f): high-resolution spectra of N 1s for etched passivation film.

hydrogen bonding with S and N atoms. The other peak at 531.5 eV (O2) may be attributed to Cu_2O on the coating surface. Besides, O 1s almost disappears after Ar^+ sputtering etching for 10 min.

The high-resolution S 2p spectrum are shown in Fig. 4d and can be decomposed into four components at binding energies of 162.8 eV, 164.1 eV, 164.3 eV and 165.5 eV. Comparing the S 2p spectra of MBT molecules, it is found that the binding energy of S atoms in the endocylic remains unchanged, while the binding energy of S atoms of the exocyclic increases by 0.80 eV, the existence of the binding energy at 162.8 eV strongly indicates that a chemical bond is formed between Cu and the exocyclic S atom in the MBT molecule.[5,28,29] Fig. 3e shows that only one main peak with the binding energy of 399.4 eV is present in the N 1s spectrum of the composite passivation film. Some studies believe that N 1s peak in the Cu–BTA complex product exhibits a delocalized effect, and the charge difference of the three N is erased.[30,31] Therefore, it is speculated that the signal of N 1s peak mainly comes from the MBT molecule. The presence of S 2p and N 1s spectra indicated that the molecularly adsorbed MBT exists on the surface of the composite passivation film.

In addition, Fig. 5 shows the photoelectron spectrum of Cu 2p and Cu LM2 Auger transitions for the composite passivation film. As shown in Fig. 5a, there is no obvious shake-up satellites

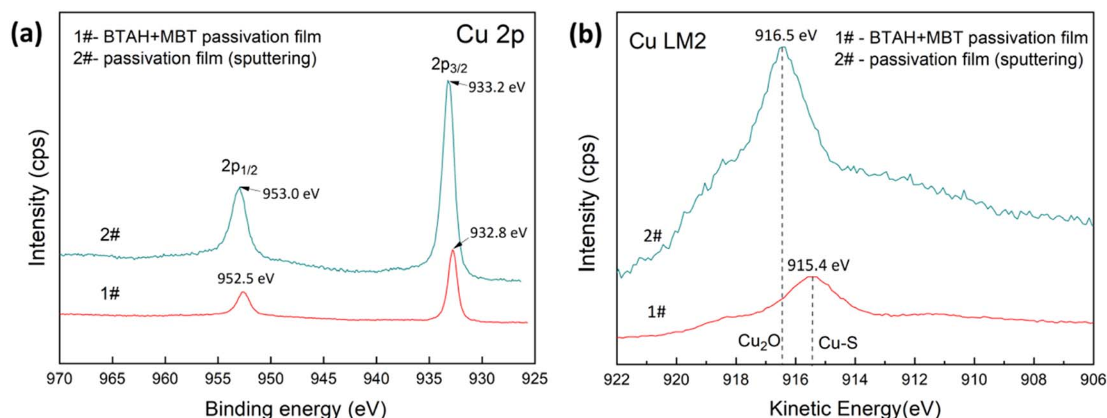

Fig. 5 Cu 2p full spectrum (a) and Cu LM2 high-resolution spectrum (b) of BTAH + MBT passivation film on the copper coating surface.

 © 2022 The Author(s). Published by the Royal Society of Chemistry

between Cu 2p1/2 peak and Cu 2p3/2 peak, indicating that the products of Cu(II) is absent on the surface of the composite passivation film.[5] However, the Cu 2p spectrum cannot distinguish the Cu atom in Cu_2O and thiolate Cu–S bond as these peaks almost overlap.[5,32] The Cu LM2 Auger transition provides basic information about the oxidation state of Cu. For the composite passivation film, an Auger characteristic peak can be observed at the kinetic energy of 915.4 eV, which may be attributed to the complex formed between MBT and Cu(I).[5,29] Combined with the analysis of O 1s spectrum, it can be determined that MBT-Cu(I) and Cu_2O are present on the surface of the passivation film.

However, O 1s almost disappears if the passivation film is etched by Ar^+ for 10 min, seen in Fig. 4a, showing that Cu_2O is absent in the inner layer of passivation film. Furthermore, Cu LM2 Auger peak appears at a kinetic energy of 916.5 eV, indicating the existence of thiolate Cu–S bonds.[5,29] Fig. 4f also shows that the N 1s spectrum of the etched composite passivation film can be fitted into two peaks with binding energies of 398.9 eV (N2) and 400.4 eV (N3), which correspond to the N atom of BTAH and MBT, respectively. Based on the analysis of Cu LM2 and N 1s peaks, it can be considered that the inner layer of the composite passivation film is mainly composed of BTA-Cu (I) and MBT-Cu (I).

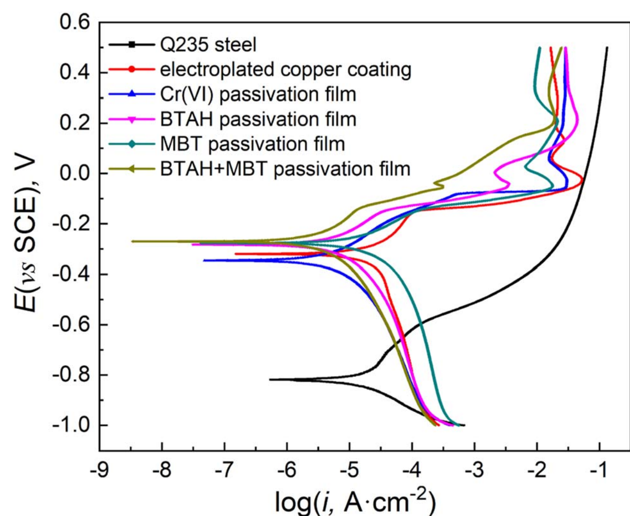

Fig. 6 Potentiodynamic polarization curves of Q235 steel, unpassivated copper coating and copper coating treated by different passivation system in 3.5% NaCl solution.

Open Access Article. Published on 25 October 2022. Downloaded on 1/31/2025 4:54:28 AM.
This article is licensed under a Creative Commons Attribution-NonCommercial 3.0 Unported Licence.

3.4 Evaluation of corrosion resistance of passivation film on the surface of copper coating

Fig. 6 gives the potentiodynamic polarization curves of copper coatings with different passivation treatments in 3.5% NaCl solution, and Table 2 shows the corresponding fitting results. The corrosion resistance of Q235 steel is very poor, and its corrosion current density (i_{corr}) is as high as 84.12 μA cm^{-2}. Due to the high density and certain protective effect of the copper coating, its corrosion current density is slightly lower than that of Q235 steel, but the overall corrosion resistance is not good. After the copper coating is passivated by BTAH, MBT, BTAH + MBT or Cr(VI), its corrosion electrochemical process in NaCl solution is inhibited to a certain extent, especially for the inhibition of anodic dissolution, and the corrosion current density is significantly reduced. By comparison, it can be found that the polarization resistance of copper coating treated by BTAH + MBT composite passivation is the largest (9185 Ω cm^2), the corrosion current density is only 1/10 of the untreated coating and the corrosion inhibition efficiency reaches 90.7%, showing the better corrosion resistance. The corrosion resistance of the coating treated by single MBT is relatively poor, which is related to the low compactness of the simple adsorption layer and the existence of a few holes in the film. In addition, Fig. 6 shows that all polarization curves have a Cu(I) oxidation peak around 0 mV, and the oxidation peak becomes significantly smaller after passivation treatment, the oxidation peak almost disappeared for the samples treated with BTAH + MBT composite passivation. In summary, BTAH and MBT have obvious synergistic effects on copper coatings, and the combined action of the two substances forms a complete and dense passivation film, which makes the composite passivation film show better corrosion resistance than the two used alone, and also better than the hexavalent chromium passivation film.

Fig. 7 shows the electrochemical impedance spectra of copper coatings with different passivation treatments in 3.5% NaCl solution. As shown in Fig. 7a, the impedance spectrum of bare copper coating exhibits a capacitive loop at high-frequency and a low-frequency at Warburg impedance. The impedance characteristics of copper coatings are quite different after different passivation treatments. Although the copper coatings treated by BTAH and hexavalent chromium passivation still show Warburg impedance in the low frequency region, the radius of capacitive arc in the high frequency has a significant difference. While, the copper coating passivated by MBT shows an inductive arc in the low frequency region (Fig. 7b), and the

Table 2 Electrochemical corrosion data of copper coatings treated by different passivation system

Samples	E_{corr} (V)	i_{corr} (μA cm^{-2})	R_p(Ω cm^2)	η (%)
Q235 steel	−0.8200	84.12	2996.3	—
Electroplated copper coating	−0.3207	44.23	1363.6	—
Cr(VI) passivation film	−0.3472	5.472	5729.7	87.63
BTAH passivation film	−0.2811	7.325	4839.2	83.44
MBT passivation film	−0.2766	17.36	1767.8	61.97
BTAH + MBT passivation film	−0.2670	4.111	9185.0	90.71

Open Access Article. Published on 25 October 2022. Downloaded on 1/31/2025 4:54:28 AM.
This article is licensed under a Creative Commons Attribution-NonCommercial 3.0 Unported Licence.

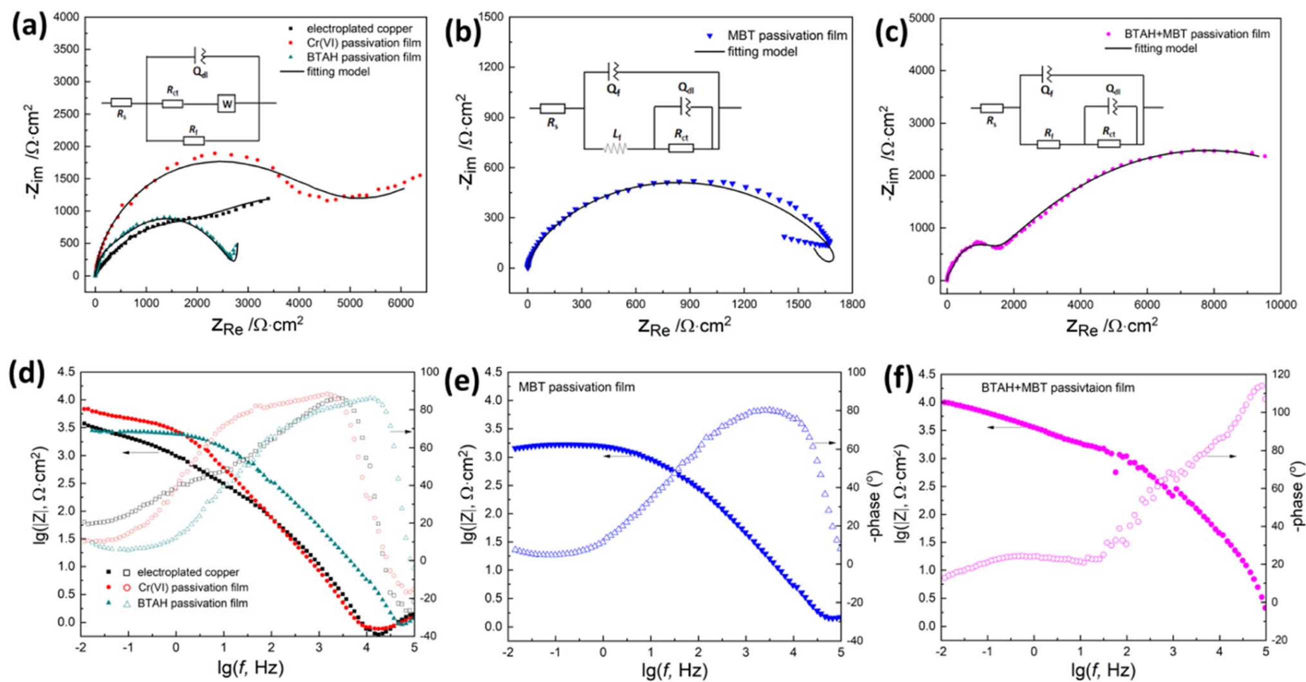

Fig. 7 Nyquist polts (a–c) and Bode plots (d– f) of electroplated copper coatings treated by different passivation system in 3.5% NaCl solution.

EIS diagram of the copper coating after BTAH + MBT composite passivation shows the double capacitive arc (Fig. 7c).

In general, the high frequency region of EIS diagram represents the barrier properties of the film, the low frequency region reflects the control steps of corrosion process, and the profile of EIS diagram is closely related to the microstructure of the film.[3,5,33–35] It is inferred that the corrosion of bare copper coating is controlled by the diffusion process of oxygen in the coating, and its corrosion behavior can be simulated using the equivalent circuit R(Q(RW)R).[16,36] BTAH passivation and hexavalent chromium passivation do not change the corrosion process of copper coating, but the formation of a passivation film on the surface can effectively isolate the copper coating from the solution, thereby reducing the corrosion rate of the coating.[1,11,15–17,30] Moreover, the coverage of a single BTAH passivation film is not complete, and the isolation effect is significantly worse than that of the hexavalent chromium passivation film. For MBT-passivated copper coatings, the appearance of inductive arc may be related to the corrosion inhibition mechanism of MBT. MBT mainly prevents the corrosion of copper coating by chemical adsorption on the surface of copper coating[5,12,18–20] But the simple adsorption layer is not dense and has a few holes (see Fig. 2h), and so the corrosion reaction easily occurs at the defect site of the MBT film, resulting in pitting corrosion.[16,24,37] Here, the equivalent circuit of R(Q(L(QR))) can be used to simulate the corrosion process. However, a complete and uniform passivation film including BTA-Cu(I) complex products and MBT-Cu(I) adsorbates is formed on the surface of copper coating after composite passivation treatment by BTAH + MBT. The composite passivation film can effectively prevent the diffusion of dissolved oxygen on the electrode surface and has a good protective effect on the copper coating. At this time, the corrosion process has been transformed into electrochemical reaction control, and the equivalent circuit of R(Q(R(RQ))) can be used to simulate this corrosion process.[5,18,33,35]

In the circuit, R_s is the solution resistance, R_{ct} and Q_{dl} represent the charge transfer resistance and the double-layer capacitance at the interface of copper coating/passivation film, R_f and Q_f reflect the resistance and the constant phase element of passivation film, L_f is the inductance exhibited by the adsorption of MBT corrosion inhibitor molecules, and Z_W represents the required diffusion resistance that dissolved oxygen reached the coating surface.[18,19,37] Generally, R_{ct} can

Table 3 Fitting results of impedance spectra for copper coating treated by different passivation system in 3.5% NaCl solution

Samples	R_f/Ω cm^2	Q_f/F cm^{-2}	n_f	R_{ct}/Ω cm^2	Q_{dl}/F cm^{-2}	n_{dl}	Y_w/Ω^{-1} cm^{-2} s$^{1/2}$	L_f/H cm^{-2}
Electroplated copper coating	—	—	—	1727	2.296×10^{-4}	0.6022	0.00241	—
Cr(VI) passivation film	5969	6.824×10^{-5}	0.6522	2651	5.298×10^{-5}	0.3541	0.00596	—
BTAH passivation film	1030	2.012×10^{-5}	0.6677	2333	4.996×10^{-5}	0.8148	0.00944	—
MBT passivation film	126	5.662×10^{-5}	0.5346	1776	1.772×10^{-4}	~1.0	—	7.545×10^{-5}
BTAH + MBT passivation film	7974	1.140×10^{-5}	0.7728	4580	1.296×10^{-5}	~1.0	—	—

 © 2022 The Author(s). Published by the Royal Society of Chemistry

reflect the corrosion reaction resistance, R_f and n_f can illustrate the protection effect and integrity of the passivation film.[33–35,37] The electrochemical impedance spectra of different passivation films are fitted according to the relevant circuits, and the results are shown in Table 3.

As shown in Table 3, the film resistance R_f is introduced into the surface of copper coating after passivation treatment, and the R_{ct} value is also significantly improved, which shows that the adsorption film or complex product film formed by the passivation treatment has a significant inhibitory effect on the corrosion of copper coating.[5,18,19,24,33–35,37] However, the electrochemical information parameters (R_f, Q_f and n_f) of the copper coatings with different passivation treatments are quite different. In contrast, MBT and BTAH composite passivation film has relatively higher R_f and n_f value, that is, the passivation film has higher density and greater corrosion reaction resistance. The R_f and n_f value of the hexavalent chromium passivation film are second. The R_f and n_f value of the single MBT passivation film are the smallest, indicating that the integrity of the passivation film is poor and the improvement on the corrosion resistance of copper coating is limited. In addition, since the dielectric constant of organic compounds is lower than that of water, the existence of organic adsorption films or complex films significantly reduces the electric double layer capacitance (Q_{dl}) value, and the film capacitance (Q_f) value also has significant differences due to the integrity of different passivation films.[10–12,30,34,37]

In summary, a layer of MBT molecular adsorption layer or thiolate (Cu–S) adsorbate will be formed on the surface of copper coating after passivation treatment with MBT solution, but the simple adsorption layer is not dense and has poor corrosion resistance. In the BTAH solution, the surface of copper coating will react with BTAH to form a Cu(I)–BTA complex protective film, which increases the reaction resistance to a certain extent and improves the corrosion resistance. In the composite passivation system, not only an organic compound adsorption film is formed on the surface of copper coating, but also a complex product film is present under the synergistic effect of BTAH and MBT. The coverage and compactness of the passivation film are greatly improved, which effectively hinders the migration of corrosive media and provides better corrosion resistance.

3.5 Discussion on synergistic passivation mechanism of BTAH and MBT on copper coatings

According to the evolution law of the surface potential (Fig. 1) and microscopic morphology (Fig. 2 and 3), and the chemical composition of the film (Fig. 4) during the composite passivation process of MBT and BTAH, it can be inferred that the formation process of the passivation film in the BTAH + MBT composite system is divided into four stages: chemical dissolution of copper plating, preferential adsorption of MBT, the formation of Cu(I)–BTA complex product film and Cu_2O, and co-promotion of Cu(I)–BTA complex film and Cu(I)–MBT adsorption film. Based on the above analysis, a growth model of BATH and MBT composite passivation film on the surface of electroplated copper coating is proposed and schematically presented in Fig. 8.

The electroplated copper coating belongs to the epitaxial growth, the crystal grain reaches the level of nm, and its chemical activity is high.[10,38] As illustrated in Fig. 8a, when the copper coating is immersed in the composite passivation solution of

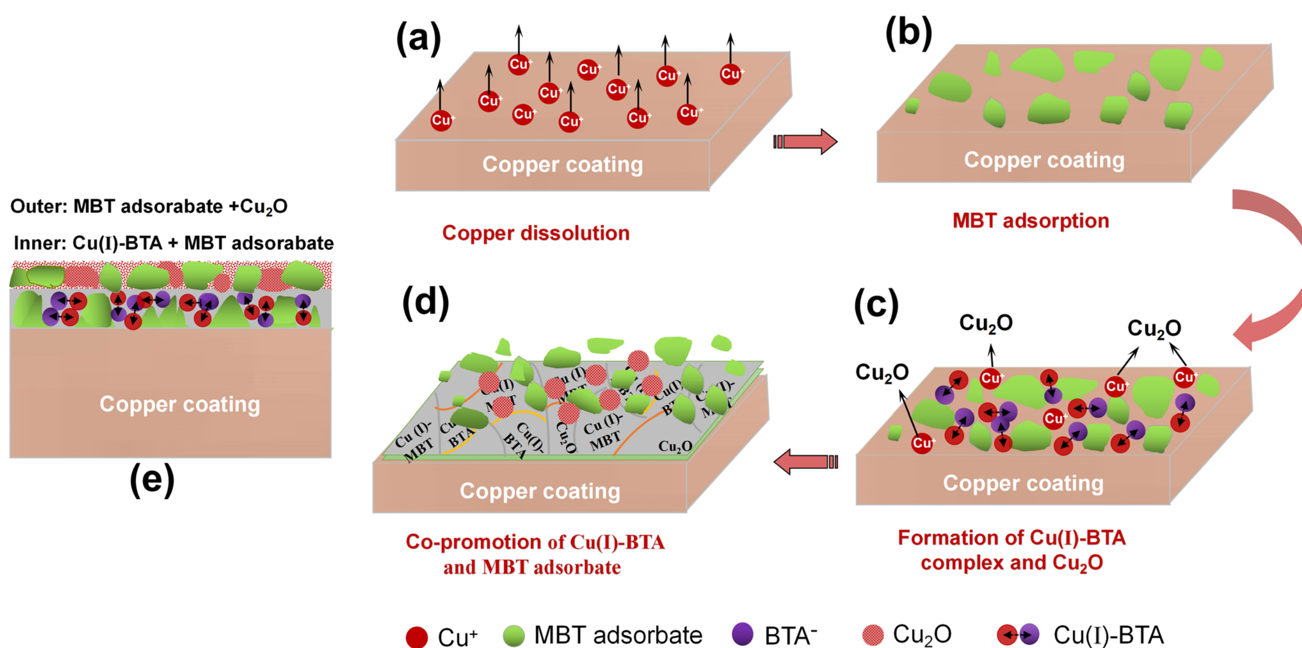

Fig. 8 Growth model of passivation film for electroplated copper coating in BATH + MBT composite system at different stages: (a) dissolution of copper coating; (b) preferential adsorption of MBT; (c) formation of Cu(I)–BTA complex and Cu_2O; (d) co-promotion of Cu(I)–BTA and MBT adsorbate; (e) structure diagram of passivation film.

Open Access Article. Published on 25 October 2022. Downloaded on 1/31/2025 4:54:28 AM. This article is licensed under a Creative Commons Attribution-NonCommercial 3.0 Unported Licence.

Open Access Article. Published on 25 October 2022. Downloaded on 1/31/2025 4:54:28 AM.
This article is licensed under a Creative Commons Attribution-NonCommercial 3.0 Unported Licence.

BTAH and MBT, the anodic active dissolution of copper will rapidly occur, seen in eqn (2); meanwhile, the copper oxide (Cu_2O) that existed on the coating surface will also be chemically dissolved, seen in eqn (3), which leads to a rapid decay of the electrode potential.[5,11,39] The surface potential of copper coating decreased from −0.364 V to −0.429 V within 17 s.

$$Cu - e^- \rightarrow Cu^+ \quad (2)$$

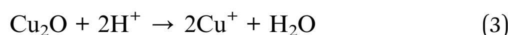

$$Cu_2O + 2H^+ \rightarrow 2Cu^+ + H_2O \quad (3)$$

MBT molecule contains S element, and the S-containing base heterocyclic compounds are easily adsorbed at the Cu/solution interface through forming stable coordination bonds between the lone pair electrons of S atom and Cu^0 and Cu^+ on the surface of copper electrode.[5,12,18,24] The S atoms in the MBT molecule preferentially chemisorb with copper and form a Cu(I)–MBT film when the copper coating is immersed in the composite passivation solution,[5,12,18,20,24] as depicted in Fig. 8b. Meanwhile, MBT can also be adsorbed on the surface of copper coating in the form of thiolate (Cu–S bond).[5,12,20] The chemical adsorption of MBT molecules will effectively block the corrosion of copper coating, but the MBT adsorption film is incomplete.

Since the MBT adsorption film cannot completely prevent the dissolution of the copper coating, the Cu^+ can react with BTAH in the composite passivation solution to form a Cu(I)–BTA complex protective film when Cu^+ concentration in the system reaches a high level. It is believed that BTAH molecules in alkaline aqueous solutions is predominantly present in the form of BTA^-, seen in eqn (4).[11,40] Meanwhile, the π* orbital energy level of BTAH molecule is low and is easy to accept electrons from the full Cu*(d) orbital to form a π feedback bond, thereby forming a stable [Cu(I)–BTA] complex film, as shown in eqn (5).[11,22,39] However, only a small part (about 8%) of monovalent copper on the surface of copper electrode participates in the formation of [Cu(I)–BTA], and most of the monovalent copper may react with dissolved oxygen to form Cu_2O, two relations can be written as eqn (6).[17,41] This process can be expressed by Fig. 8c.

$$BTAH \rightleftarrows BTA^- + H^+ \quad (4)$$

$$Cu(I) + BTAH \rightarrow Cu(I)\text{–}BTA + H^+ \quad (5)$$

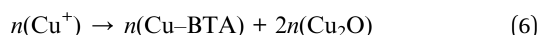

$$n(Cu^+) \rightarrow n(Cu\text{–}BTA) + 2n(Cu_2O) \quad (6)$$

The formation speed of [Cu(I)–BTA] complex film is slow due to the limited number of monovalent copper ions, and so the complex film has many defects. At this time, MBT molecules can still form a passivation film at the defect of [Cu(I)–BTA] complex film through strong chemical adsorption. Under the mutual promotion of BTAH and MBT, the [Cu(I)–BTA] complex film and Cu(I)–MBT adsorption film are continuously formed and gradually cover the entire coating, and so a denser protective film is formed on the surface of the coating, seen in Fig. 8d, thereby inhibiting the corrosion of copper coating. In the later stage, the dissolution reaction of Cu^+ is difficult to occur, and the adsorption of MBT becomes dominant until it reaches saturation.

Based on this effect, a bilayer protective film, containing the inner layer of BTA–Cu(I) and MBT–Cu(I) and the outer layer of MBT–Cu(I) and Cu_2O, is formed on the surface of electroplated copper coating after the composite passivation treatment by BTAH and MBT. The schematic diagram of this bilayer film is shown in Fig. 8e. It effectively hinders the corrosion of copper coating and improves its corrosion resistance.

4 Conclusions

(1) A bilayer protective film can be formed on the surface of the electroplated copper coating after treatment by BTAH and MBT composite passivation solution. XPS analysis results show that the main composition of the inner layer are BTA–Cu(I) and MBT-Cu(I), the main composition of outer layer are MBT–Cu(I) and Cu_2O, and the thickness of the passivation film is about 233 nm.

(2) The formation process of BTAH and MBT composite passivation film on the surface of electroplated copper coating includes: chemical dissolution of copper coating, preferential adsorption of MBT, formation of Cu(I)–BTA complex product film and Cu_2O, and co-promotion of Cu(I)–BTA and Cu(I)–MBT.

(3) BTAH and MBT composite passivation treatment greatly inhibits the anodic dissolution process of the copper coating, significantly improves its corrosion resistance, and is far better than the effect of BTAH or MBT alone, or even better than the hexavalent chromium passivation. The self-corrosion current density of copper coating after composite passivtion of MBT and BTA is only 1/10 of that of the untreated coating.

Conflicts of interest

There are no conflicts to declare.

Acknowledgements

The authors gratefully acknowledge the support of Major Discipline Academic and Technical Leaders Training Program of Jiangxi Province (No. 20204BCJL23033), Natural Science Foundation of Jiangxi, China (No. 20212BAB204043), and Jiangxi Postgraduate Innovation Fund (No. YC2021–S654).

References

1 Ž. Z. Tasić, M. B. Petrović Mihajlović, M. B. Radovanović and M. M. Antonijević, New trends in corrosion protection of copper, *Chem. Pap.*, 2019, **73**, 2103–2132.

2 S. Hong, S. You, A. Fu, Z. Shi, H. Xie, D. Cao, C. J. Lin, G. Fu, L. S. Zheng, Y. Jiang and N. Zheng, Surface coordination layer passivates oxidation of copper, *Nature*, 2020, **586**, 390–394.

3 Y. Ma, B. Fan, H. Liu, G. Fan, H. Hao and B. Yang, Enhanced corrosion inhibition of aniline derivatives electropolymerized coatings on copper: preparation,

© 2022 The Author(s). Published by the Royal Society of Chemistry

Open Access Article. Published on 25 October 2022. Downloaded on 1/31/2025 4:54:28 AM.
This article is licensed under a Creative Commons Attribution-NonCommercial 3.0 Unported Licence.

characterization and mechanism modeling, *Appl. Surf. Sci.*, 2020, **514**, 146086.

4 Y. Li, H. Yang, F. Wang and Y. Huang, Fabrication and anticorrosion properties of melamine-treated graphene oxide adsorbed on copper, *Prog. Org. Coat.*, 2020, **141**, 105564.

5 Y. Tao, X. Chen, S. Peng and Y. Ma, The enhancement and mechanism of potential-assisted method on 2-mercaptobenzobthiazole assembled film for copper protection, *Colloids Surf., A*, 2022, **638**, 128280.

6 M. Scardamaglia, V. Boix, G. D. 'Acunto, C. Struzzi, N. Reckinger, X. Chen, A. Shivayogimath, T. Booth and J. Knudsen, Comparative study of copper oxidation protection with graphene and hexagonal boron nitride, *Carbon*, 2021, **171**, 610–617.

7 L. Hurley Belinda and L. McCreery Richard, Raman spectroscopy of monolayers formed from chromate corrosion inhibitor on copper surfaces, *J. Electrochem. Soc.*, 2003, **150**, B367–B373.

8 Q. J. Wang, M. S. Zheng and J. W. Zhu, Semi-conductive properties of passive films formed on copper in chromate solutions, *Thin Solid Films*, 2009, **517**, 1995–1999.

9 C. T. Wang, S. H. Chen, S. Y. Zhao and D. G. Li, Inhibition effect of allylthiourea and 1-dodecanethiol on copper corrosion, *Acta Chim. Sin.*, 2003, **61**, 151–155.

10 Y. S. Tan, M. P. Srinivasan and S. O. Pehkonen, Self-assembled organic thin films on electroplated copper for prevention of corrosion, *J. Vac. Sci. Technol., A*, 2004, **22**, 1917–1925.

11 M. Fingar and I. Miloev, Inhibition of copper corrosion by 1,2,3-benzotriazole: A review, *Corros. Sci.*, 2010, **52**, 2737–2749.

12 L. P. Kazansky, I. A. Selyaninov and Y. I. Kuznetsov, Adsorption of 2-mercaptobenzothiazole on copper surface from phosphate solutions, *Appl. Surf. Sci.*, 2012, **258**, 6807–6813.

13 H. Tavakoli, T. Shahrabi and M. G. Hosseini, Synergistic effect on corrosion inhibition of copper by sodium dodecylbenzenesulphonate (SDBS) and 2-mercaptobenzoxazole, *Mater. Chem. Phys.*, 2008, **109**, 281–286.

14 D. Gelman, D. Starosvetsky and Y. Ein-Eli, Copper corrosion mitigation by binary inhibitor compositions of potassium sorbate and benzotriazole, *Corros. Sci.*, 2014, **82**, 271–279.

15 D. Q. Zhang, H. G. Joo and K. Y. Lee, Investigation of molybdate–benzotriazole surface treatment against copper tarnishing, *Surf. Interface Anal.*, 2009, **41**, 164–169.

16 S. Liu, J. Dong, W. W. Guan, J. M. Duan, R. Y. Jiang, Z. P. Feng and W. J. Song, The synergistic effect of Na_3PO_4 and benzotriazole on the inhibition of copper corrosion in tetra-n-butylammonium bromide aerated aqueous solution, *Mater. Corros.*, 2012, **63**, 1017–1025.

17 T. Yang, W. Chen, X. Li, J. Song, L. Dong and Y. Q. Fu, Environment-friendly and chromium-free passivation of copper and its alloys, *Mater. Today Commun.*, 2021, **29**, 102826.

18 M. Finšgar and D. K. Merl, An electrochemical, long-term immersion, and XPS study of 2-mercaptobenzothiazole as a copper corrosion inhibitor in chloride solution, *Corros. Sci.*, 2014, **83**, 164–175.

19 S. B. Sharma, V. Maurice, L. H. Klein and P. Marcus, Local inhibition by 2-mercaptobenzothiazole of early stage intergranular corrosion of copper, *J. Electrochem. Soc.*, 2020, **167**, 161504.

20 E. Vernack, D. Costa, P. Tingaut and P. Marcus, DFT studies of 2-mercaptobenzothiazole and 2-mercaptobenzimidazole as corrosion inhibitors for copper, *Corros. Sci.*, 2020, **174**, 108840.

21 M. Sugimasa, L. J. Wan, J. Inukai and K. Itaya, Adlayers of benzotriazole on Cu (110), (100), and (111) in $HClO_4$ solution: *in situ* scanning tunneling microscopy study, *J. Electrochem. Soc.*, 2002, **149**, E367.

22 F. Grillo, D. W. Tee, S. M. Francis, H. A. Früchtl and N. V. Richardson, Passivation of copper: benzotriazole films on Cu(111), *J. Phys. Chem.*, 2014, **C118**, 8667–8675.

23 S. Peng, Z. Zeng, W. Zhao, J. Chen, J. Han and X. Wu, Performance evaluation of mercapto functional hybrid silica sol-gel coating on copper surface, *Surf. Coat. Technol.*, 2014, **251**, 135–142.

24 M. Finšgar, 2-Mercaptobenzimidazole as a copper corrosion inhibitor: part I. Long-term immersion, 3D-profifilometry, and electrochemistry, *Corros. Sci.*, 2013, **72**, 82–89.

25 X. Zhang, C. van den Bos, W. G. Sloof, A. Hovestad, H. Terryn and J. H. W. de Wit, Comparison of the morphology and corrosion performance of Cr(VI)- and Cr(III)-based conversion coatings on zinc, *Surf. Coat. Technol.*, 2005, **199**, 92–104.

26 H. P. King and L. E. Alexander, *X-ray Diffraction Procedures for Polycrystalline and Amorphous Materials*, 2nd edn, NewYork, Wiley, 1974.

27 M. Finšgar, 2-Mercaptobenzimidazole as a copper corrosion inhibitor: part II. Surface analysis using X-ray photoelectron spectroscopy, *Corros. Sci.*, 2013, **72**, 90–98.

28 L. P. Kazansky, Y. E. Pronin and I. A. Arkhipushkin, XPS study of adsorption of 2-mercaptobenzothiazole on a brass surface, *Corros. Sci.*, 2014, **89**, 21–29.

29 R. Woods, G. A. Hope and K. Watling, A SERS spectroelectrochemical investigation of the interaction of 2-mercaptobenzothiazole with copper, silver and gold surfaces, *J. Appl. Electrochem.*, 2000, **30**, 1209–1222.

30 T. Hashemi and C. A. Hogarth, The mechanism of corrosion inhibition of copper in NaCl solution by benzotriazole studied by electron spectroscopy, *Electrochim. Acta*, 1988, **33**, 1123–1127.

31 K. Mansikkamaki, U. Haapanen, C. Johans, K. Kontturi and M. Valden, Adsorption of benzotriazole on the surface of copper alloys studied by SECM and XPS, *J. Electrochem. Soc.*, 2006, **153**, B311–B318.

32 P. E. Larson, X-ray induced photoelectron and auger spectra of Cu, CuO, Cu_2O, and Cu_2S thin films, *J. Electron Spectrosc. Relat. Phenom.*, 1974, **3**, 213–218.

33 M. E. Orazem and B. Tribollet, *Electrochemical Impedance Spectroscopy*, 1st edn Wiley, John & Sons, Incorporated, 2008.

34 P. Wang, C. Liang, B. Wu, N. Huang and J. Li, Protection of copper corrosion by modification of dodecanethiol self-

Open Access Article. Published on 25 October 2022. Downloaded on 1/31/2025 4:54:28 AM.
This article is licensed under a Creative Commons Attribution-NonCommercial 3.0 Unported Licence.

assembled monolayers prepared in aqueous micellar solution, *Electrochim. Acta*, 2010, **55**, 878–883.

35 S. X. Wang, X. H. Liu, L. Q. Wang, Q. J. Wen, N. Du and J. H. Huang, Formation mechanism and properties of fluoride–phosphate conversion coating on titanium alloy, *RSC Adv.*, 2017, **7**, 16078–16086.

36 A. Palit and S. O. Pehkonen, Copper corrosion in distribution systems: evaluation of a homogeneous Cu_2O film and a natural corrosion scale as corrosion inhibitors, *Corros. Sci.*, 2000, **42**, 1801–1822.

37 M. Finšgar and D. K. Merl, 2-Mercaptobenzoxazole as a copper corrosion inhibitor in chloride solution: electrochemistry, 3D-profifilometry, and XPS surface analysis, *Corros. Sci.*, 2013, **80**, 82–95.

38 J. Zheng, H. Chen, W. Cai, L. Qiao, Y. Ying, W. Li, J. Yu, L. Jiang and S. Che, Reaction mechanisms of copper electrodeposition from 1-hydroxyethylidene-1,1-diphosphonic acid (HEDP) solution on glassy carbon, *Mater. Sci. Eng., B*, 2017, **224**, 18–27.

39 V. Brusic, M. A. Frisch, B. N. Eldridge, F. P. Novak, F. B. Kaufman, B. M. Rush and G. S. Frankel, Copper corrosion with and without inhibitors, *J. Electrochem. Soc.*, 1991, **138**, 2253–2259.

40 M. Scendo and J. Malyszko, Influence of benzotriazole and tolyltriazole on the copper electrodeposition on polycrystalline platinum from acidic chloride solutions, *J. Electrochem. Soc.*, 2000, **147**, 1758–1762.

41 W. Qafsaoui, C. Blanc, N. Pébère, H. Takenouti, A. Srhiri and G. Mankowski, Quantitative characterization of protective films grown on copper in the presence of different triazole derivative inhibitors, *Electrochim. Acta*, 2002, **47**, 4339–4346.

© 2022 The Author(s). Published by the Royal Society of Chemistry